

Influence of catalysts on the rate of crystallization and on the crystal distortions in poly(ethylene terephthalate)

TSUTOMU ASANO*, ASTRID DZEICK-PICKUTH,
HANS GERHARD ZACHMANN
*Institut für Technische und Makromolekulare Chemie, Universität Hamburg,
2000 Hamburg 13, FRG*

The crystallization behaviour of poly(ethylene terephthalate) (PET) containing different amounts of catalysts as well as of PET without catalysts has been studied. The kinetics of crystallization from the glassy state has been investigated by time-resolved small-angle X-ray scattering employing synchrotron radiation. The degree of crystallinity and Ruland's lattice distortion factor k were measured by wide-angle X-ray scattering. The results show that not only calcium acetate but also manganese acetate acts as a nucleating agent in PET. If the crystallization takes place close to the glass transition temperature, the catalysts also influence the amount of lattice distortions: the larger the nucleating effect, the smaller the factor k . This is explained by the fact that, due to restricted motion of the molecules, the amount of lattice distortion of the crystals within a spherulite increases with increasing distance from the centre of the spherulite.

1. Introduction

Poly(ethylene terephthalate) (PET) is easily obtained in a glassy amorphous state by quenching from the melt. The mechanism of crystallization from the glassy state has been of much interest for a long time. The density change during crystallization was measured by Keller *et al.* [1-3] and by Zachmann and Stuart [4]. Günther and Zachmann [5] studied the influence of catalysts on the kinetics of crystallization. Yeh and Geil [6] investigated the initial stage of the crystallization by electron microscopy. The effect of molecular orientation on the crystallization behaviour was studied by Althen and Zachmann [7] and by Alfonso *et al.* [8].

By employing synchrotron radiation, it became possible to perform time-resolved measurements of small-angle X-ray scattering (SAXS) during crystallization [9]. This new method was applied first by Elsner *et al.* [10] for studies of the kinetics of crystallization of industrial samples of PET.

The degree of crystallinity and the lattice distortion factor can be determined by means of wide-angle X-ray scattering (WAXS) using the evaluation method of Ruland [11, 12]. This method has been applied to PET by Gehrke and Zachmann [13] and by Vonk [14]. A method for the investigation of oriented samples has been developed by Bösecke and Zachmann [15, 16].

In the present study, the mechanism of crystallization of PET from the glassy state is examined by time-resolved SAXS studies and by WAXS measurements. The method of Ruland with a slight change in the procedure of evaluation is applied for determi-

nation of the degree of crystallinity and the lattice distortion factor from the WAXS curves. The effect of catalysts and of molecular orientation on the lattice distortions and on the kinetics of crystallization is of prime interest.

2. Experimental procedure

2.1. Preparation of the samples

The PET samples were synthesized from terephthalic acid dimethylester and ethylene glycol as described by Günther and Zachmann [5]. 0.0288 mol % antimony trioxide and 0.112 mol % calcium acetate or manganese acetate were added as catalysts. The temperatures and times of polycondensation and the molecular weight obtained, M_w , are shown in Table I.

In addition, a PET sample was synthesized from oligo(ethylene terephthalate) without a catalyst. The oligomer was heated stepwise in a vacuum of 1.3 Pa and finally kept at 285°C for 3.5 h. The change of temperature during the synthesis is shown in Fig. 1. The molecular weight obtained, M_w , was 35 000 g mol⁻¹.

As indicated in Table I, we designate in the following

TABLE I Description of the samples investigated

Sample	Catalyst	Polycondensation		Molecular weight (g mol ⁻¹)
		Temperature (°C)	Time	
M	Manganese acetate	270	30 min	33 000
C	Calcium acetate	270	45 min	33 000
O	No catalyst	285	3.5 h	35 000

* Permanent address: Department of Physics, Faculty of Science, Shizuoka University, Shizuoka 422, Japan.

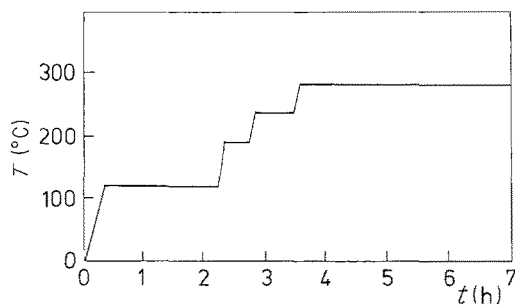


Figure 1 Temperature T as a function of time t during synthesis of PET without catalysts *in vacuo* ($p = 1.3$ Pa).

the sample containing calcium acetate by C, that containing manganese acetate by M, and the sample without catalyst by O.

The synthesized samples were melt-pressed to films and then quenched in ice-water. In some cases the samples were oriented by homogeneous drawing at 86°C . The molecular orientation is characterized by the birefringence Δn_0 .

2.2. Experimental methods

The kinetics of crystallization was studied by means of SAXS employing synchrotron radiation at HASYLAB in DESY, Hamburg. The amorphous samples, which were held between two metal plates so that shrinkage was not possible, were rapidly introduced into a furnace which was kept at the crystallization temperature. The SAXS intensity was measured as a function of crystallization time by means of a position-sensitive linear counter. The intensity of the primary beam was determined by using a semi-transparent beam stop [17].

As described earlier [10, 18], during the process of spherulite growth the scattering power Q , i.e. the intensity integrated over all angles, is proportional to the volume of the spherulites and, consequently, to the degree of crystallinity. Therefore, the half-time of crystallization and the Avrami constant could be evaluated from the increase of Q .

In the case of the oriented samples, the linear counter was positioned in such a way that the scattering was measured along the meridian. As is known [19], the azimuthal half-width of the SAXS reflection decreases during crystallization. This causes an additional increase in the scattering power on the meridian.

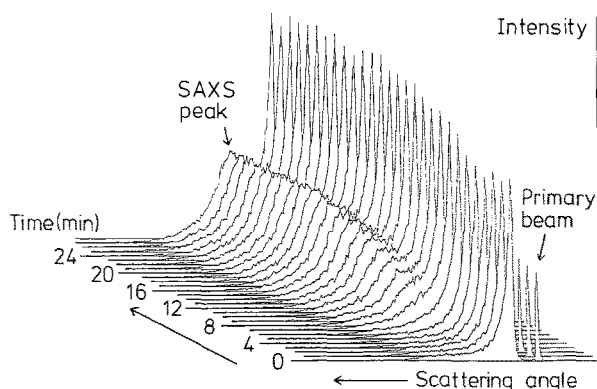


Figure 2 Change of the SAXS pattern of Sample C during crystallization from the glassy state at 110°C .

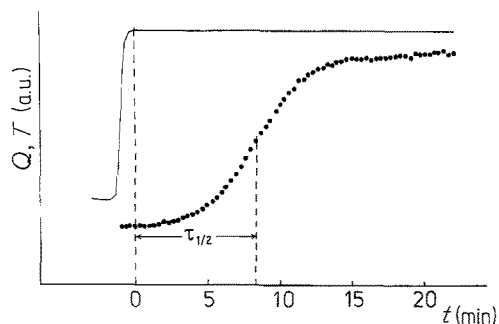


Figure 3 (●) Scattering power Q and (—) temperature T as a function of time t during crystallization of Sample C at 110°C .

Therefore, in order that our evaluation be correct, we have to assume that, to a first approximation, the change in the azimuthal half-width is proportional to the change in the degree of crystallinity.

The degree of crystallinity and the amount of lattice distortion were obtained from WAXS patterns which were measured by means of a Siemens D500 goniometer at room temperature. The scattered intensity was detected by the usual proportional counter. In order to get good resolution, we chose the time of the measurement at each angle in such a way that we obtained a fixed count rate of 2×10^4 counts sec^{-1} . An Apple computer was used for data treatment. The results were evaluated by means of the method of Ruland, applying the slightly changed procedure described in Section 3.2.

The density was measured by a density gradient column at 23°C filled with hexane/tetrachloromethane. From the density, a degree of crystallinity was calculated assuming that the density of the crystals is given by $\rho_c = 1.495$ g cm^{-3} and that of the amorphous regions by $\rho_a = 1.334$ g cm^{-3} .

3. Results

3.1. SAXS measurements

Fig. 2 shows as an example the change of the SAXS pattern of Sample C with time during crystallization at 110°C . One can clearly recognize that the peak intensity increase with time. In Fig. 3 the change of the scattering power Q obtained by integration of the

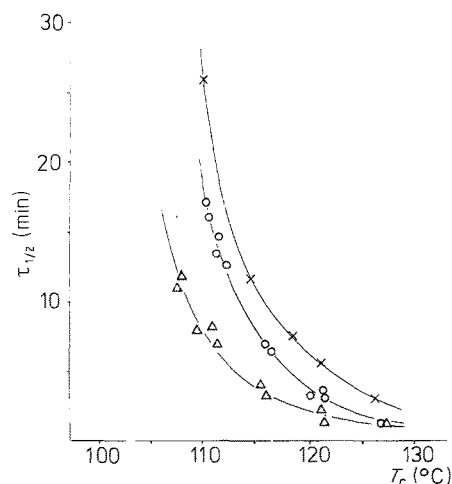


Figure 4 Half-time of crystallization $\tau_{1/2}$ of the unoriented samples as a function of the crystallization temperature T_c . (Δ) Sample C, (\circ) Sample M, (\times) Sample O.

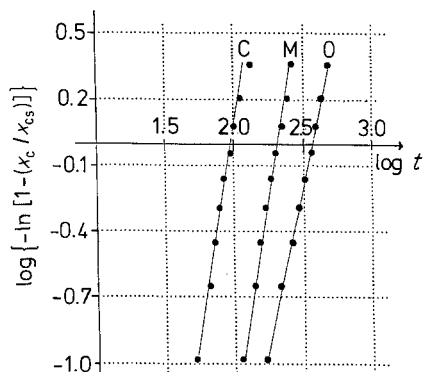


Figure 5 Avrami plot of the results on kinetics of crystallization at $T_c = 121^\circ\text{C}$.

scattered intensity over all angles is represented. Q increases until a constant degree of crystallinity is reached. From the change of Q , the half-time of crystallization, $\tau_{1/2}$, was determined.

Fig. 4 represents $\tau_{1/2}$ as a function of the crystallization temperature T_c for all samples investigated. As can be seen, the catalysts reduce the half-time of crystallization considerably. Calcium acetate has a greater effect than manganese acetate, which is in agreement with previous observations [5].

The Avrami exponent n and the Avrami constant G were evaluated from the Avrami equation

$$x_c(t) = x_{cs}[1 - \exp(-G \cdot t^n)] \quad (1)$$

where $x_c(t)$ is the degree of crystallinity at time t and x_{cs} is the final degree of crystallinity. The ratio $x_c(t)/x_{cs}(t)$ is equal to $Q(t)/Q_e$, the ratio of the scattering powers at time t and at the end of crystallization, respectively. In Fig. 5, $\log\{-\ln[1 - (x_c/x_{cs})]\}$ is plotted as a function of $\log t$ for a crystallization temperature $T_c = 121^\circ\text{C}$. By evaluation of such curves, we have determined n from the slopes of the straight line and G from the intercept on the ordinate. The results are summarized in Table II. With the unoriented samples, values of the Avrami exponent n of about 3 are observed. In the case of slightly oriented samples (birefringence $\Delta n_0 = 10 \times 10^{-3}$), the half-time is smaller than in the undrawn sample, while n is still about 3. At higher orientation ($\Delta n_0 = 17 \times 10^{-3}$) the Avrami exponent n decreases to about 2, indicating that the features of the crystallization differ from those of the undrawn samples.

TABLE II Parameters of crystallization kinetics

Sample	Birefringence, Δn (10^3)	Crystallization temperature ($^\circ\text{C}$)	Half-time, $\tau_{1/2}$ (sec)	Avrami exponent, n	Avrami constant, G (sec^{-1})
C	0	110.9	417	2.95	1.0×10^{-8}
M	0	110.9	955	3.34	8.1×10^{-11}
O	0	109.8	1549	2.83	6.4×10^{-10}
C	0	121.0	85	2.83	1.0×10^{-7}
M	0	121.0	186	3.35	1.6×10^{-8}
O	0	120.9	324	2.89	3.7×10^{-8}
M	10	113.0	310	3.40	1.6×10^{-9}
M	17	100.0	470	2.05	2.6×10^{-6}
M	17	105.0	210	1.75	6.6×10^{-5}

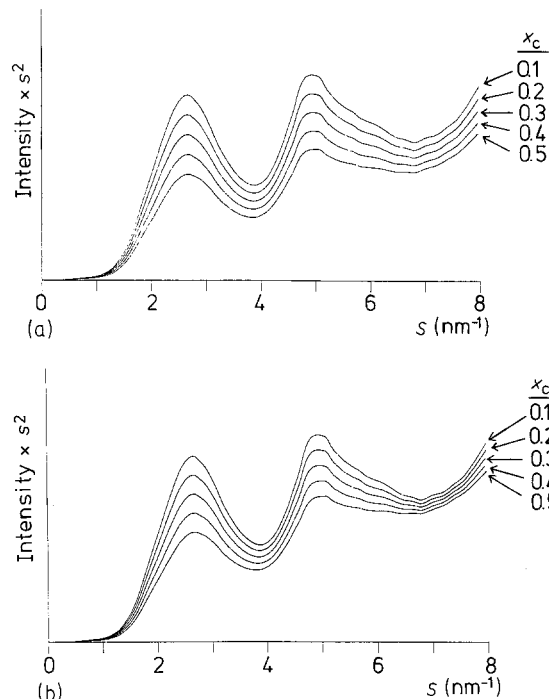


Figure 6 Normalized background scattering caused by the amorphous regions and crystal imperfections for various values of the degree of crystallinity x_c and for two different values of k : (a) $k = 0.01$, (b) $k = 0.02$.

3.2. WAXS measurements

The degree of crystallinity and the lattice distortion factor were determined by evaluation of the WAXS pattern. The measured curves were corrected for the air scattering, the polarization factor and the absorption factor, and then multiplied by s^2 ($s = 2 \sin \theta / \lambda$ with θ being half the scattering angle and λ the wavelength). The curves were normalized by adding the atomic scattering factor for the coherent scattering, $f_{\text{coh}}^2(s)$, and for the Compton scattering, $f_{\text{inc}}^2(s)$, averaged over the different atoms. Then the Compton scattering was subtracted.

For the further evaluation of the X-ray scattering curve the method of Ruland [11–14] has been slightly modified, resulting in the following procedure: a background scattering caused by the amorphous regions and the crystal imperfections has been calculated by means of the equation

$$s^2 I_{\text{back}} = x_c s^2 f_{\text{coh}}^2(s) [1 - \exp(-ks^2)] + (1 - x_c) s^2 I_{\text{amorph.}}(s) \quad (2)$$

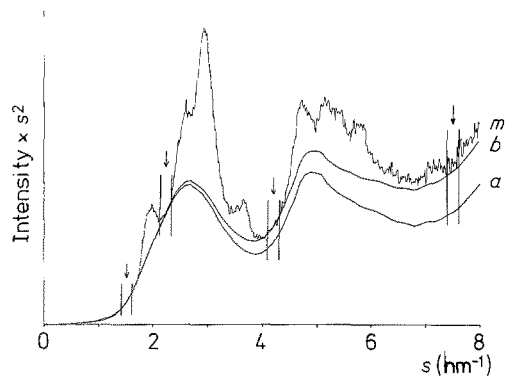


Figure 7 Measured scattering m , calculated background scattering b and amorphous scattering a of Sample M crystallized for 80 min at $T_c = 130^\circ\text{C}$.

where x_c is the crystallinity, $f_{\text{coh}}^2(s)$ is the averaged atomic scattering factor for coherent scattering, and k is the distortion factor of the first-order lattice distortion [11–13]. The first term of Equation 2 is the contribution from the diffuse scattering of the distorted crystal. Different values for x_c and k were assumed for the calculation. The second term is the amorphous scattering, where $I_{\text{amorph.}}(s)$ is measured from a quenched PET sample.

Fig. 6a shows the background scattering calculated in the case of $k = 0.01$, assuming different degrees of crystallinity varying from 0.1 to 0.5. Fig. 6b shows the corresponding results in the case of $k = 0.02$. As one can recognize, an increase of the degree of crystallinity at a constant value of k causes the background curves to shift downwards, while increasing values of k lead to an increase of the scattering intensity at high values of s .

In order to evaluate the measured WAXS curves of the different samples, the calculated curves were fitted to the measured ones. In order to do so, the crystallinity x_c and the lattice distortion factor k of the calculated WAXS curve were varied until the best fit was obtained over those regions of the measured WAXS curve in which scattering arises only from the amorphous regions and the crystal distortions. We chose the four intervals $s = 1.4$ to 1.6 , $s = 2.1$ to 2.3 , $s = 4.0$ to 4.2 and $s = 7.4$ to 7.6 nm^{-1} , as these fitting regions, in agreement with previous results (see Fig. 3 in [13]). x_c and k were determined as the values giving the best fit.

The result for Sample M crystallized at 130°C for 80 min is shown in Fig. 7. The best fit of the background curve is obtained at $x_c = 0.32$ and $k = 0.022$. Consequently the scattering of the amorphous regions in Fig. 7 is obtained by multiplying the normalized intensity measured with a quenched sample of PET by a factor of 0.68. The difference between the background scattering and that of the amorphous regions is attributed to the lattice distortion.

Fig. 8 shows the WAXS curves of Sample M crystallized for different times at 130°C . The degree of crystallinity becomes larger with increasing crystallization time. The fitting regions are marked by arrows. In the region $s = 1$ to 5 nm^{-1} the scattered intensity is lowered with increasing crystallization time, but all curves are at the same level in the region $s > 6 \text{ nm}^{-1}$. This result shows that the amount of lattice distortion becomes larger with increasing crystallization time.

Fig. 9 represents the WAXS curves for different samples all crystallized at 110°C for 60 min. The

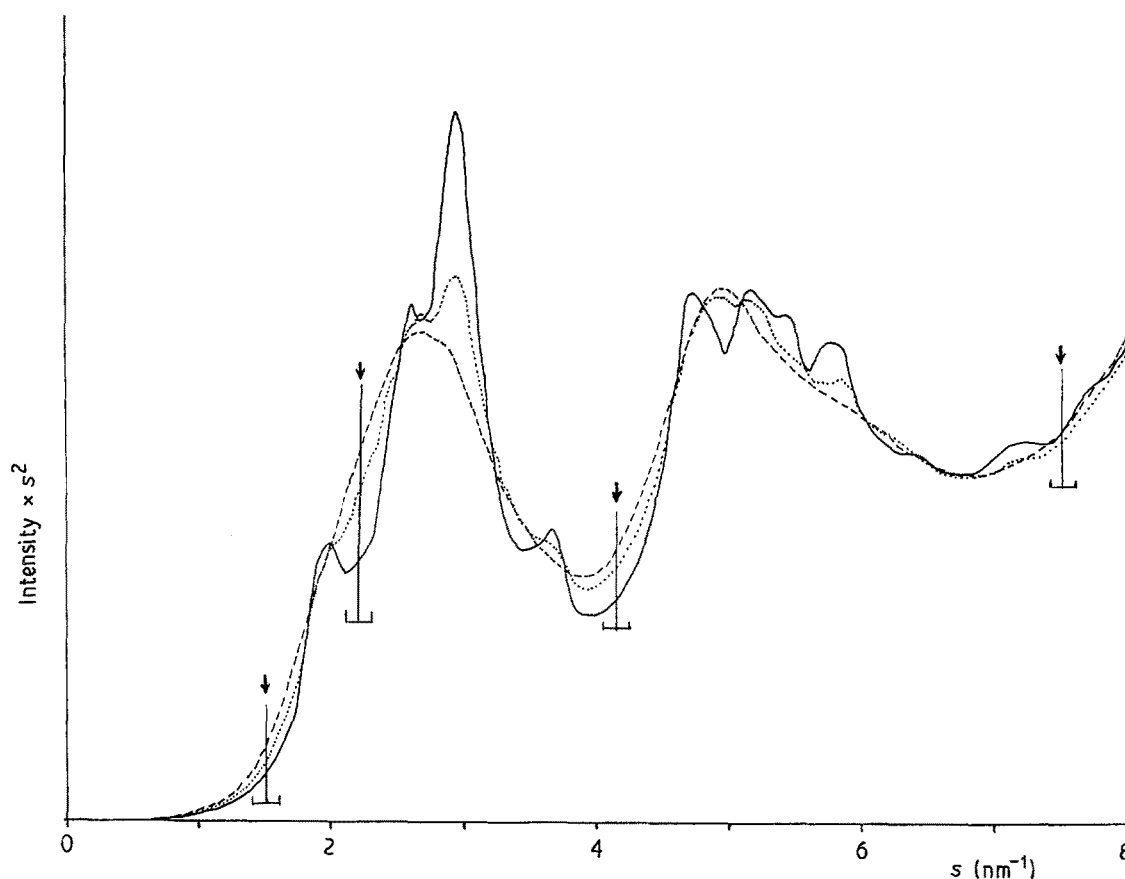


Figure 8 Normalized WAXS curves of Sample M crystallized at 130°C for (---) 60 sec, (···) 80 sec and (—) 80 min.

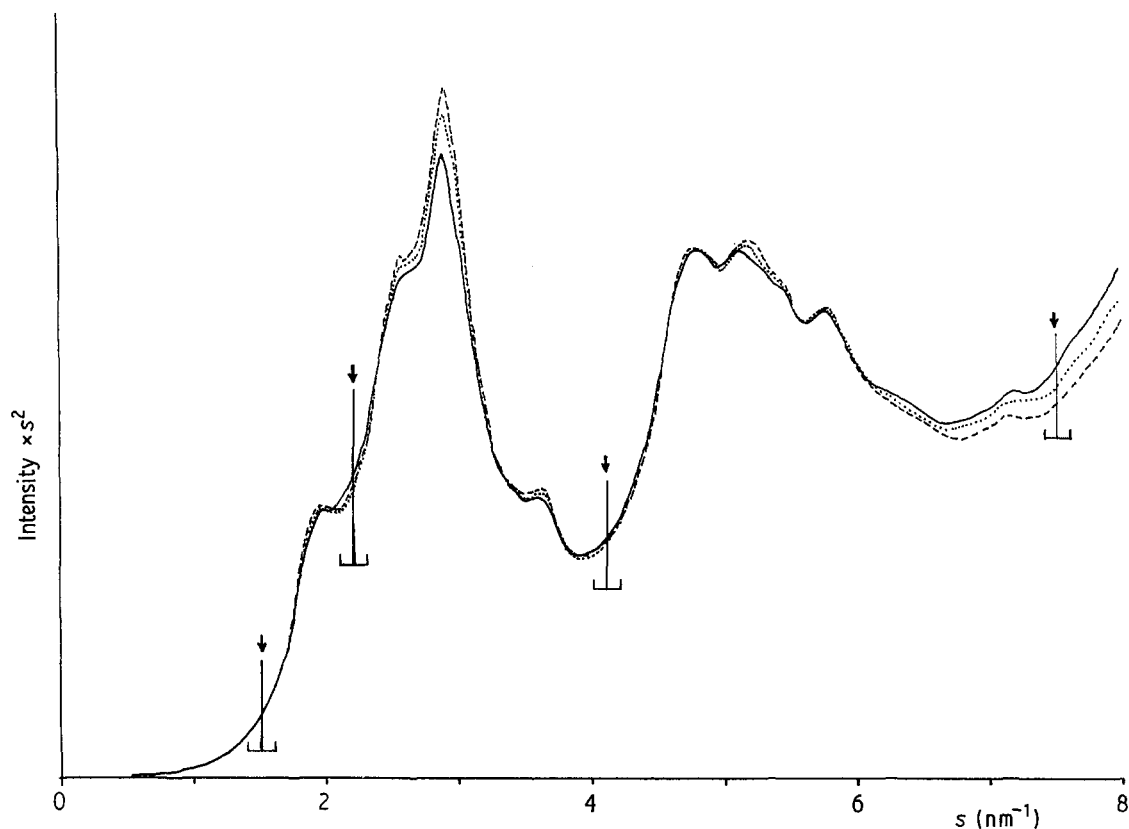


Figure 9 Normalized WAXS curves of (—) Sample O, (· · ·) Sample M, and (---) Sample C.

degrees of crystallinity are nearly the same for all samples. However, large differences in the scattered intensity at $s > 6 \text{ nm}^{-1}$ are observed. This indicates that the amount of lattice distortion is smallest in the sample with calcium acetate, medium in the sample with manganese acetate and largest in the sample without catalyst.

The effect of the crystallization temperature T_c is demonstrated in Fig. 10. An increase in crystallinity

with increasing T_c is observed. The scattered intensity at $s > 6 \text{ nm}^{-1}$ is smallest for $T_c = 150^\circ \text{C}$, which indicates that the amount of lattice distortion is smallest at this crystallization temperature.

The results of a quantitative evaluation of the WAXS measurements are summarized in Table III together with the density measurements: With all samples it is observed that the lattice distortion factor k becomes larger with increasing crystallization time.

TABLE III Degree of crystallinity, lattice distortion factor and density of samples crystallized under different conditions

Sample	Birefringence, $\Delta n (\times 10^3)$	Crystallization		Crystallinity (WAXS), x_c	Lattice distortion, $k (\text{nm}^2)$	Density $\rho (\text{g cm}^{-3})$	Crystallinity (density), x_ρ
		Temperature ($^\circ \text{C}$)	Time				
C	0	130	10 sec	0.09	0.003	1.346	0.06
C	0	130	20 sec	0.22	0.016	1.369	0.22
C	0	130	80 min	0.33	0.022	1.377	0.28
M	0	130	60 sec	0.05	0.009	1.346	0.06
M	0	130	80 sec	0.11	0.016	1.356	0.13
M	0	130	80 min	0.32	0.022	1.383	0.32
O	0	130	150 sec	0.04	0.010	1.346	0.06
O	0	130	300 sec	0.22	0.022	1.365	0.19
O	0	130	80 min	0.32	0.022	1.377	0.28
C	0	110	60 min	0.28	0.016	1.374	0.26
M	0	110	60 min	0.27	0.018	1.372	0.24
O	0	110	60 min	0.23	0.020	1.364	0.19
C	0	125	60 min	0.33	0.020	1.380	0.30
M	0	125	60 min	0.33	0.025	1.378	0.29
O	0	125	60 min	0.33	0.025	1.376	0.27
C	0	150	60 min	0.36	0.013	1.383	0.32
M	0	150	60 min	0.36	0.013	1.383	0.32
O	0	150	60 min	0.37	0.013	1.382	0.31
C	10	110	300 sec	0.22	0.013	1.366	0.20
M	10	110	300 sec	0.26	0.016	1.367	0.21
O	10	110	300 sec	0.22	0.022	1.366	0.20

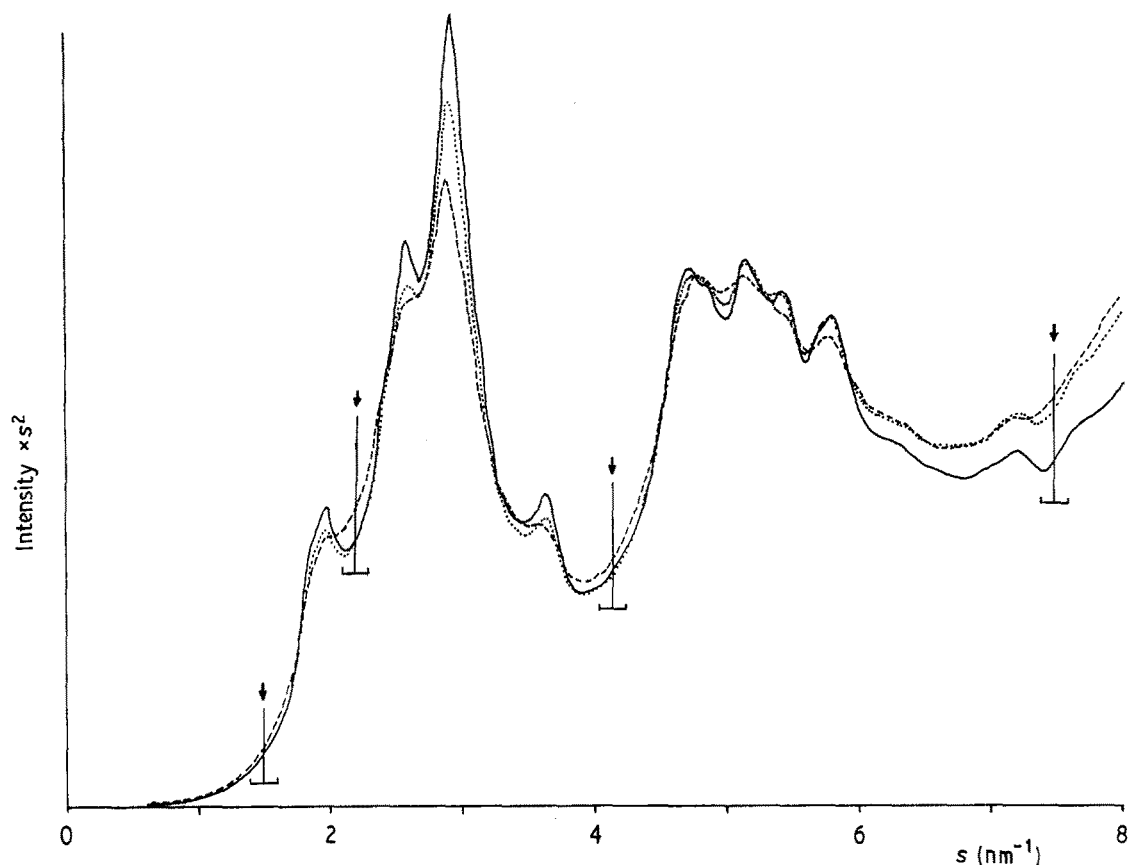


Figure 10 Normalized WAXS curves of sample O crystallized for 60 min at (---) 110°C, (···) 125°C and (—) 150°C.

In the case of crystallization at $T_c = 110$ and 125°C , one obtains the lowest value of k for Sample C and the highest one for Sample O. In the case of $T_c = 150^\circ\text{C}$, k has the same value for all samples which is much smaller than after crystallization at $T_c = 110$ and 125°C . Finally, with slightly oriented samples ($\Delta n_0 = 10 \times 10^{-3}$), one observes the same influence of the catalyst on the lattice distortions as with the unoriented ones.

The change of the lattice distortion factor k as a function of the degree of crystallinity x_c is shown in Fig. 11. In all the samples, the lattice distortions become larger with increasing degree of crystallinity up to $x_c = 0.3$ and then decrease. In the region of increase of k , Sample C shows the lowest value of k while Sample O shows the highest value.

4. Discussion

4.1. Influence of the catalysts on the crystallization rate

Previous results have shown that a PET sample containing calcium acetate as a catalyst crystallizes much faster than one containing manganese acetate [5]. This was attributed to the fact that calcium acetate acts as a nucleation agent. In the present work, by measuring in addition the rate of crystallization of samples without catalysts, it is shown that manganese acetate, too, acts as a nucleation agent, though to a lesser extent than calcium acetate.

It is worthwhile to note that the nucleating agent influences the rate of crystallization even at comparatively low temperatures close to the glass transition. Usually, one tends to assume that crystal

nucleation is no problem in this region because the critical crystal nucleus is comparatively small. The small rate of crystallization is attributed to the small mobility of the molecules. Our results show, however, that the rate of nucleation is still of great influence.

The Avrami exponent n is not affected by the catalysts within the error of the experiments. For PET containing catalysts, n equals 3 as for the material which is free of catalysts.

4.2. Amount of lattice distortion

If the crystallization takes place at 130°C , the lattice distortion factor k increases with increasing crystallization time. After crystallization at 125 and 110°C , the value of k strongly depends on the catalyst: it is largest for the sample containing no catalyst, smaller for the sample containing manganese acetate and smallest for the sample containing calcium acetate.

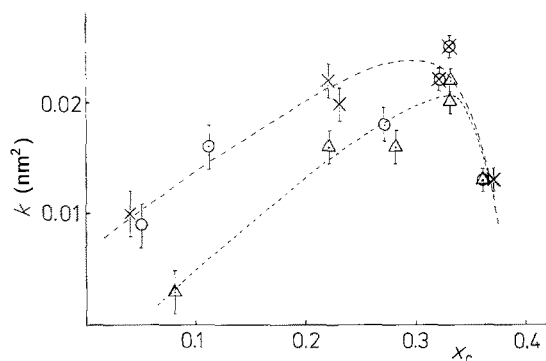


Figure 11 Lattice distortion factor k as a function of the degree of crystallinity x_c : (Δ) Sample C, (\circ) Sample M, (\times) Sample O.

Thus, the larger the nucleation effect, the smaller the value of k . This behaviour can be explained in the following way.

In the process of crystallization, the molecular packing is changed leading to an increase of the density. In order to accomplish this, the molecules have to move. At temperatures near the glass transition, the molecular mobility is limited and the displacements of the segments cannot take place as completely as necessary in order to build up perfect crystals. However, the amount of displacement depends on the location of the crystal. After the growth of a spherulite has started from one nucleus, the lateral shift of the molecules increases with increasing distance from that nucleus. Therefore, the more lattice distortion the crystals contain, the further away from the centre of the spherulite they are located.

By means of these considerations, we can explain the increase of lattice distortion with crystallization time by the fact that the radii of the spherulites become larger with time. The catalyst is of influence because it reduces the size of the spherulites. The effect of the catalyst is also observed in the oriented sample, where fibrils instead of spherulites grow from each nucleus.

The size of the spherulites only affects the lattice distortions at crystallization temperature near T_g (at 130°C and below). If the sample is crystallized at 150°C, k does not depend on the catalyst (see Table III) and is considerably smaller than after crystallization at 130°C. Furthermore, at $T_c = 206^\circ\text{C}$ the lattice distortion factor k decreases during crystallization from 0.025 to 0.015 nm² within 10 min [13]. We therefore conclude that, at higher crystallization temperatures, the mobility of the molecules is so large that lattice distortions formed during crystallization can be healed by relaxation effects. Thus, we have two competing processes:

- (i) an increase of lattice distortions due to increasing distance from the nucleation centre, and
- (ii) the thermal relaxation which decreases the lattice distortion.

At low temperatures, the first effect is strong because of the limited thermal motion. At higher temperatures, the second process which occurs simultaneously with the first one is of greater importance.

Acknowledgements

The authors are very much indebted to Dr S. L. Kim and Dr D. Smith from the Goodyear Tire and Rubber Co., Akron, Ohio, for the supply of oligo(ethylene terephthalate) without catalysts. One of the authors (T.A.) gratefully acknowledges that Shizuoka University, Japan, has granted him leave of absence for studies in Germany. This work has been funded by the German Federal Minister for Research and Technology (BMFT) under Contract No. 05305 HXB.

References

1. A. KELLER, G. R. LESTER, L. B. MORGAN, F. D. HARTLEY and E. W. LORD, *Phil. Trans. R. Soc.* **A247** (1954) 1.
2. *Idem.*, *ibid.* **A247** (1954) 13.
3. *Idem.*, *ibid.* **247** (1954) 23.
4. H. G. ZACHMANN and H. A. STUART, *Makromol. Chem.* **41** (1960) 131.
5. B. GÜNTHER and H. G. ZACHMANN, *Polymer* **24** (1983) 1008.
6. G. E. YEH and P. H. GEIL, *J. Macromol. Sci.* **B1** (1967) 235.
7. G. ALTHEN and H. G. ZACHMANN, *Makromol. Chem.* **180** (1979) 2723.
8. G. C. ALFONSO, M. P. VERDONA and A. WASIAK, *Polymer* **19** (1978) 711.
9. G. ELSNER, C. RIEKEL and H. G. ZACHMANN, *Adv. Polym. Sci.* **67** (1985) 1.
10. G. ELSNER, M. H. J. KOCH, J. BORDAS and H. G. ZACHMANN, *Makromol. Chem.* **182** (1981) 1263.
11. W. RULAND, *Acta Crystallogr.* **14** (1961) 1180.
12. *Idem.*, *Polymer* **5** (1964) 89.
13. R. GEHRKE and H. G. ZACHMANN, *Makromol. Chem.* **182** (1981) 627.
14. C. G. VONK, *J. Appl. Crystallogr.* **6** (1973) 148.
15. P. BÖSECKE, Diploma thesis, University of Hamburg (1984).
16. P. BÖSECKE and H. G. ZACHMANN, to be published.
17. H. G. ZACHMANN, D. WISWE, R. GEHRKE and C. RIEKEL, *Macromol. Chem. Suppl.* No. **12** (1985) 175.
18. H. G. ZACHMANN and R. GEHRKE, 'Morphology of Polymers', edited by B. Sedlacek (de Gruyter, Berlin, 1986).
19. G. ELSNER and H. G. ZACHMANN, *Makromol. Chem.* **182** (1981) 657.

Received 18 February
and accepted 14 June 1988